SUPERPLASTICIZER–NANOSILICA COMPATIBILITY: ASSESSMENT AND OPTIMIZATION

Harry Brace and Emilio Garcia-Taengua

Biography:

Harry Brace is a Graduate Engineer at Ramboll UK Ltd in Cambridge (England). He obtained his MEng in Civil and Structural Engineering from the University of Leeds (England). His research interests include special concretes, rheology of cement-based materials, and the interactions between chemical admixtures and additions.

ACI member **Emilio Garcia-Taengua** is Assistant Professor at the School of Civil Engineering, University of Leeds (England). He received his MEng in Civil Engineering, MSc in Applied Statistics and PhD in Concrete Technology from the Universitat Politècnica de València (Spain). He is a member of ACI Committees 237 (Self-Consolidating Concrete), 240 (Nanotechnology), and 544 (Fiber-Reinforced Concrete) and RILEM Committee 261-CCF (Creep of FRC). His research interests include bond, creep, nanotechnology, and optimization of special concretes.

ABSTRACT

Nanoparticles can yield significant benefits in cement-based products but can pose problems regarding dispersion and optimal doses. This paper proposes an inexpensive methodology to compare superplasticizers in terms of their compatibility with nanosilica, providing concrete technologists with a practical tool to select the best combinations. A series of cement pastes were produced, incorporating nanosilica and two different superplasticizers at different dosages. Their fresh state performance was assessed by means of the Marsh funnel test, and their compressive strength was determined at 28 days. The compatibility between nanosilica and superplasticizers was defined and described by developing semi-empirical models. These were used to identify optimal combinations which maximize the flowability and compressive strength and minimize their variability. It was concluded that the optimization of cement pastes with nanosilica was feasible only when the superplasticizer used is highly compatible. Careful selection of the superplasticizer proved to be critical in ensuring the efficiency and cost-effectiveness of the addition of nanosilica.

Keywords: chemical admixtures; compatibility; compressive strength; fresh state performance; Marsh funnel test; paste; statistical models.

INTRODUCTION

Supplementary cementitious materials (SCMs) like fly ash, silica fume or ground granulated blast-furnace slag are by-products of other industrial processes that can be incorporated to cement-based mixes. They have attracted considerable interest and have been increasingly used for two main reasons. Firstly, an increasing interest in special concretes such as self-consolidating concrete or high performance concrete, which incorporate significantly greater amounts of powders other than cement[1–3]. Secondly, the encouragement of reducing the energy consumption associated with cement production[4]. Continuous efforts to develop new SCMs have widened the range of possibilities to produce concrete with tailored properties. One of the most interesting areas of current development is nanotechnology, as anticipated by Feynman[5], largely thanks to technical improvements allowing for greater manipulation at the nanoscale[6]. Some of the most interesting examples are nano-Fe_2O_3, nano-TiO_2, and nanosilica (NS). These can yield different characteristics, such as improved mechanical performance in the case of NS or photocatalytic properties in the case of nano-TiO_2[6–8].

NS consists of ultrafine particles of amorphous silica, which is available as a powder or predispersed in the form of a slurry or hydrosol[9], and partakes in the cement hydration processes[10]. The majority of articles published so far dealing with the applications of nanotechnology in construction materials are concerned with NS, and it has been reported as the most widely used variety of nanoparticles[11,12]. However, the difficulties associated to its effective dispersion in fresh cementitious systems have been the major hindrance to their introduction in large scale concrete production.

Nanosilica and cement hydration

NS has a positive impact on cement hydration and can enhance density, strength development and mechanical properties of cement-based materials[12–16]. Its reactivity is explained by its high purity in terms of SiO_2 content and its high specific surface area[6,17]. It increases the rate of cement hydration reactions, as confirmed by the correlation between NS content and the release of heat of hydration[12,18].

NS contributes to the enhancement of mechanical properties of cement-based materials through three main mechanisms of action[18]: its pozzolanic activity, the filler effect, and NS particles providing nucleation sites for cement hydration products. It acts as a pozzolan as it reacts with the calcium hydroxide to form additional C-S-H[12,18]. Furthermore, NS particles can fill voids, which results in a lower capillary porosity, refined microstructure and higher strength[19,20], and act as nucleation sites for the hydration products, outperforming silica fume[19].

As a result, the addition of NS can improve the compressive, tensile, and flexural strength of concrete[12,15,18]. Establishing the range of NS contents that maximize the aforementioned properties is crucial to its introduction in the concrete manufacturing industry. Concerning compressive strength, improvements of up to 15% have been reported, although there is significant variation in the literature[12]. The optimal NS contents required to maximize compressive strength differ significantly among different studies, ranging from 1% to 5%[15,21]. These discrepancies have been attributed to a number of factors such as differences in particle size or the production method, but the main issue seems to be the dispersion of NS particles in fresh cementitious mixes[18,22].

Nanosilica and the rheology of cement-based materials

The introduction of NS has been correlated with reduced workability, which is attributable to NS either directly or through its interaction with the type and dosage of superplasticizer[18,21,23]. This is a consequence of the high specific surface area of NS and the interactions between NS particles and the chemical species that dissolve in the liquid phases of fresh cement-based mixes[24]. The high specific surface area makes NS very reactive and allows it to provide nucleation sites during hydration, however it also results in attraction forces between particles, causing agglomeration[12]. If the particles are not well dispersed, strength gains are minimal[17,22]. Several strategies have been proposed to reduce dispersion problems, making changes to the mixing regime as well as through the use of superplasticizers. Using NS in powder form is problematic as it absorbs part of the free water in the mix[25]: colloidal preparations of NS, where NS particles are hydroxylated and monodispersed in water, are preferable. Other methods involve ultrasonication and the use of dispersants such as acetone[22]. However, NS particles still tend to reagglomerate when incorporated into the fresh mix due to the presence of Ca^{2+}, Na^{+} and K^{+} ions released from cement upon contact with water[18].

Superplasticizers have long been used to improve the rheology of fresh cementitious mixtures: they are adsorbed onto the cement particles causing deflocculation, reducing water demand and improving workability[22]. As with other additions, the introduction of NS affects the interaction between superplasticizer (SP) and cement[26] in terms of the rheology of fresh mixes, which in turn affects their hardened properties and mechanical performance. In consequence, the complex interactions between cement and NS, and between them and SPs, as well as their effect on different properties, are difficult to rationalize[27]. It is in this context that the concept of the compatibility between SP, NS and cement is introduced[26,28,29].

RESEARCH SIGNIFICANCE

This study investigates the compatibility between SPs and NS based on two simple tests which constitute a practical methodology for comparing SPs regarding their effectiveness in unlocking the potential of NS. It builds on the intuitive concept of compatibility between additions and chemical admixtures to propose a quantitative definition for the first time, making its systematic evaluation possible. Multiple linear regression is used to model the effects of NS and SP on cement pastes and to derive their optimal dosages. This methodological framework is also applicable to the study of compatibility between SPs and additions other than NS.

EXPERIMENTAL INVESTIGATION

A series of cement pastes were prepared and their performance was assessed by means of the Marsh funnel test and the uniaxial compression test. Three factors were considered: SP type, SP dosage, and NS dosage, considered at different levels of variation as summarized in **Table 1**. Two different SPs were considered: SP A and SP B. They were dosed at 0.75, 1.0, and 1.25 times their average recommended dosage, to ensure they were within their effective range. In consequence, SP A was dosed between 0.3% and 0.5% over cement weight, whilst SP B was dosed between 0.6% and 1.0%. Nanosilica was incorporated in dosages of 0.5%, 2.0% and 3.5% over cement weight, in line with previous literature suggesting that optimal dosages lie within these ranges[15,18,21]. Control pastes without NS were also produced and tested. In all cases the water-to-binder ratio was kept constant at 0.40 without using any other additions or additives. All combinations tested are shown in **Table 2**.

Materials and methods

Portland cement type CEM I 52.5N was used. The NS used was a commercially available colloidal dispersion with 40% silica by weight and an average particle size of 12 nm. The two SPs considered were selected to be representative of commercially available SPs, produced by different manufacturers, with different formulations and different ranges of recommended doses. SP A was lignosulfonate based with a typical dosage range recommended by the manufacturer between 0.2% and 0.6% by mass and a pH of 5. SP B consisted in a blend of polymers, polycarboxylate based, with a recommended dosage range between 0.3% and 1.3% by mass and a pH of 5.5.

All preparation and mixing operations were carried out in the same sequence, and the duration of all operations was the same for all pastes. An automatic, high shear mixer with a 4.5 litres [152.2 fl.oz.] capacity compliant with EN-196-2005[30] was used. First, the cement was poured into the mixing bowl and dry-mixed for 30 seconds at low speed (140 rpm). The SP and NS were premixed with the water and half of this mixture was added to the mixing bowl and mixed for 60 seconds. The mixer was stopped for 60 seconds to scrape the sides and break up any clumps. Then the rest of the water, NS and SP mixture was added and mixed for 60 seconds before the speed was increased to 285 rpm and mixed for a further 180 seconds. Finally, the speed was reduced back to 140 rpm for 30 seconds.

The flowability of all pastes was measured using the Marsh funnel test in compliance with EN 445:2007[31]. This is a relatively simple test where the time for a certain volume of paste to flow out of a funnel with standardized dimensions is measured. This parameter has been shown to provide meaningful information which can be used to determine SP dosages that are optimal from the point of view of fresh state performance[32]. To perform this test, the inner surface of the Marsh funnel was wetted to minimize surface friction. A measuring flask was placed below the funnel and its bottom was covered before it was filled with 1.2 litres [40.6

fl.oz.] of paste. For each paste, the time was measured for 1 litre [33.8 fl.oz.] to pass through the funnel, t_{1000} in seconds.

From each paste, three 50mm [1.97 in.] side cubes were produced using molds compliant with EN 196-1:2005[30]. The cubes were vibrated to ensure proper compaction and then stored at 23 °C and relative humidity of 95%. All cubes were tested under uniaxial compression at 28 days, applying the compressive load at a constant rate in compliance with EN 12390-3:2009[33]. The average compressive strength of each set of three specimens as well as the standard deviation were retained.

EXPERIMENTAL RESULTS AND ANALYSIS

Marsh funnel test results

The flow times t_{1000}, in seconds, are shown in **Table 2**. This parameter is inversely representative of the flowability of each paste: lower t_{1000} values correspond to pastes with higher flowability, whilst higher t_{1000} values correspond to thicker pastes. Multiple linear regression was applied to relate t_{1000} to the dosages of NS and SP. The equations obtained were then used to plot the response surfaces of t_{1000} with respect to the NS and SP dosages, thus allowing for a clear interpretation of the experimental results.

Having some mixes for which the t_{1000} was not measurable because of the paste not flowing through the funnel posed a problem. Considering only those mixes where t_{1000} was defined would have biased the analysis by misrepresenting the possibility of some pastes not flowing. To overcome this issue, the response parameter considered in the multiple linear regression analysis was the inverse of the flow time, $1/t_{1000}$, expressed in seconds^{-1}, instead of t_{1000}. With this transformation, in cases where the paste was too thick to flow t_{1000} was assimilated to infinity, making $1/t_{1000}$ equal to zero and therefore having quantitative values in all cases. As a result, multiple linear regression could be applied without bias to analyze the paste flowability as measured by means of the Marsh funnel test.

The multiple regression analysis yielded a very accurate model (R-squared=0.95) consisting of equations (1) and (2), depending on the SP type considered (either SP A or SP B), where t_{1000} times are expressed in seconds, and NS and SP dosages are expressed as percentage over cement weight:

$$SP\ A:\ \frac{1}{t_{1000}} = (624.8 - 271.8\ NS + 251.0\ NS \times SP) \times 10^{-4} \quad (1)$$

$$SP\ B:\ \frac{1}{t_{1000}} = (991.9 - 404.0\ NS + 251.0\ NS \times SP) \times 10^{-4} \quad (2)$$

Based on the equations above, the response surfaces for t_{1000} as a function of NS and SP dosages are shown in **Fig. 1** and **2**, for SP A and SP B respectively. In either case, the increase of the SP dosage within the recommended range had an almost negligible effect on t_{1000} when the NS content was low, whilst it yielded significant improvements in pastes with higher NS contents. For any dosage of either SP A or SP B, higher NS contents were associated with higher t_{1000} times, and the highest t_{1000} values predicted by equations (1) and (2) corresponded to those cases with low SP dosages and high NS contents, which were precisely the mixes that were too thick to flow.

To compare the performance of SP A and SP B, the response surfaces presented in **Fig. 1** and **2** could not be extended in the range of the SP axis to have them both in the same region because that would have based the comparison on extrapolation of the fitted equations outside the range each SP was tested. To make direct comparison possible between SP A and SP B, their standardized dosage SP_{std} was considered instead: –1, 0, or +1 (low, intermediate, and high dosage respectively), and equations (1) and (2) were rewritten as follows:

$$SP\ A:\ t_{1000} = 100 \times [6.93 + NS \times (0.35\ SP_{std} - 2.06)]^{-1} \quad (3)$$

$$SP\ B:\ t_{1000} = 100 \times [9.24 + NS \times (0.35\ SP_{std} - 2.06)]^{-1} \quad (4)$$

Fig. 3 shows the two response surfaces defined by equations (3) and (4) in the same plot. It is interesting to observe that both SPs had a very similar effect on the flowability when the NS content was not higher than 0.5%: on average, the difference between predicted t_{1000} values for SP A and SP B was not higher than 5 seconds. This similarity in terms of their effect on the flowability of mixes with low NS contents was attributed to the fact that their ranges of recommended dosages were well adjusted for cement pastes without NS. Also, both SP A and SP B showed similar performance in pastes with NS contents not higher than 1.5%, with differences in predicted t_{1000} values not higher than 10 seconds.

When the NS contents was higher than 1.5%, the difference between the two SPs was more pronounced. SP B yielded consistently lower t_{1000} values and therefore was better performant than SP A, when dosed within the recommended range. However, these differences are to some extent exaggerated by the scale of **Fig. 3**: both response surfaces are plotted up to a t_{1000} value of 100 seconds, whereas the experimental values obtained for t_{1000} were in no case higher than 41.8 seconds. **Fig. 4** shows these response surfaces after their intersection with a horizontal plane at t_{1000} = 40 seconds, as it was assumed that predicted t_{1000} values higher than 40 seconds represented pastes that would not flow through the funnel. The comparison between SP A and SP B could then be based on the maximum NS contents that could be added to the paste without making it unflowable. In mixes with SP A, the maximum NS content for a paste to flow through the funnel ranged between 1.7% and 2.5% (considering the SP A dosage at 0.3% or 0.5% respectively), whilst in mixes produced with SP B, the maximum NS content ranged from 2.7% to 3.5% (considering SP B dosed at 0.6% or 1.0% respectively). Therefore, the use of SP B instead of SP A allowed, on average, an extra 1.0% of NS to be added without making the paste too thick to flow through the funnel.

Considerations like those made in relation to **Fig. 4** and maximum NS contents pointed to two alternative approaches to compare the effectiveness of different SPs in cement pastes with NS. The first approach was to compare the response surfaces based on their relative positions, that is, predicted t_{1000} values being higher or lower, as discussed in relation to **Fig. 1–4**. Alternatively, the comparison could be made in terms of the boundary which separates flowable from non-flowable cases. This new approach provided additional information, and led to a systematic methodology to define the so-called region of compatibility between SP and NS, as detailed in the following section.

Compatibility between Superplasticizers and Nanosilica

As explained in the previous section, pastes that were too thick to flow through the Marsh funnel were defined as $1/t_{1000}$ = 0 seconds^{-1}, which led to equations (1) and (2). In line with this criterion, the condition $1/t_{1000} = 0$ was imposed on equations (1) and (2) to obtain the expression of the theoretical boundary separating cases of pastes that could flow through the funnel ($1/t_{1000} > 0$) from pastes that could not:

$$SP\ A:\ \ 624.8 - 271.8\,NS + 251.0\,NS \times SP = 0 \qquad (5)$$

$$SP\ B:\ \ 991.9 - 404.0\,NS + 251.0\,NS \times SP = 0 \qquad (6)$$

Fig. 5 shows equations (5) and (6) plotted in the NS-SP plane. They define the boundary of what can be called the region of theoretical compatibility between nanosilica and superplasticizer, for SP A and SP B. It can be observed that the use of SP B instead of SP A extended this region, which is consistent with the observations made in relation to **Fig. 1–4**. However, the definition of the region of compatibility could be refined by establishing an upper limit for acceptable or realistic flow times. Even though the model as given by equations (1) and (2) can yield predicted t_{1000} values in the range of zero to infinity, predicted flow times higher than a certain threshold would correspond to pastes that cannot flow through the Marsh funnel, and this is the reason why the region of compatibility defined by equations (5) and (6) has been referred to as 'theoretical'. In consistency with the experimental results, this threshold was established at 40 seconds. Furthermore, as SP A and SP B were dosed within their respective recommended ranges, which did not overlap, their standardized dosage SP_{std} was a more appropriate parameter to compare them. Considering standardized SP dosages and assuming that flowable pastes correspond to predicted $t_{1000} < 40$ seconds, the following equations were obtained:

$$SP\ A\text{:}\quad 100 \times [6.93 + NS \times (0.35\, SP_{std} - 2.06)]^{-1} < 40 \tag{7}$$

$$SP\ B\text{:}\quad 100 \times [9.24 + NS \times (0.35\, SP_{std} - 2.06)]^{-1} < 40 \tag{8}$$

Equations (7) and (8) are plotted in **Fig. 6** and define the region of true compatibility between NS and SP. These plots provided a more accurate representation of the NS-SP combinations corresponding to flowable pastes and therefore were a more refined tool for comparing SP A and SP B in terms of their compatibility with NS. In fact, the area of the compatibility regions can be used as a quantitative parameter to compare different SPs. The area of the region of true compatibility between NS and SP A was 4.2 (non-dimensional), whilst for SP B it was 6.2 (non-dimensional). In consequence, SP B turned out to be 47.6% more compatible with NS than SP A.

Average compressive strength

Compressive strength results are shown in **Table 3**. The average values were correlated with NS and SP dosages by means of multiple linear regression, and the following equations were obtained (R-squared = 0.91), where $f_{c,cube}$ stands for compressive strength expressed in MPa [conversion: 1 MPa = 145 psi]:

$$SP\ A\text{:}\quad f_{c,cube} = 25.91 + 15.08\, NS + 18.28\, SP - 2.34\, NS^2 \tag{9}$$

$$SP\ B\text{:}\quad f_{c,cube} = 40.91 + 15.08\, NS + 18.28\, SP - 2.34\, NS^2 - 5.27\, NS \times SP \tag{10}$$

The response surfaces corresponding to equations (9) and (10) are shown in **Fig. 7** and **8**, for SP A and SP B respectively. In pastes with SP A, **Fig. 7** shows that varying the SP dosage from 0.3% to 0.5% increased the average compressive strength but very slightly, only 5.7 MPa [826.5 psi] on average. On the other hand, by increasing the NS content from 0% to 3% the average compressive strength was increased in 24.2 MPa [3509 psi]. However, the relationship between compressive strength and NS content was found to follow a quadratic trend, in agreement with previous studies[18,21]: varying the NS content from 0% to 1% increased the average compressive strength in 12.7 MPa [1841.5 psi], but increasing the NS content from 2% to 3% yielded an average increase in compressive strength of only 3.4 MPa [493 psi]. Pastes produced with SP B presented compressive strength values which were on average higher than their counterparts produced with SP A, as shown in **Fig. 8**, but the relative difference between maximum and minimum values was not as pronounced as with SP A. This is more clearly seen in **Fig. 9**, where both response surfaces for compressive strength are shown together with respect to the standardized SP dosage, SP_{std}.

The NS content which maximized compressive strength was found by differentiating equations (9) and (10) with respect to NS and equalling to zero:

$$SP\ A: \quad \frac{\partial f_{c,cube}}{\partial (NS)} = 0 \rightarrow 15.08 - 4.68\,NS = 0 \rightarrow NS = 3.22\,\% \tag{11}$$

$$SP\ B: \quad \frac{\partial f_{c,cube}}{\partial (NS)} = 0 \rightarrow 15.08 - 4.68\,NS - 5.27\,SP = 0 \rightarrow NS = (3.22 - 1.13\,SP)\,\% \tag{12}$$

Equation (11) shows that the optimal NS content, in cement pastes produced with SP A, was 3.22% regardless of the SP dosage. On the other hand, for cement pastes produced with SP B, equation (12) shows that the optimal NS content was a function of the SP dosage, and it varied between 2.1% to 2.6% for the range of SP dosages considered in this study.

Variability of Compressive strength

The variability of compressive strength is usually examined through the coefficient of variation (CoV), which is the ratio between the standard deviation and the average compressive strength, in percentage, for each set of three specimens. Standard deviation and CoV values are shown in **Table 3**. CoV values were correlated with NS and SP dosages by means of multiple linear regression, and the following equations were obtained (R-squared = 0.89):

$$SP\ A:\ \ CoV = 6.51 + {SP_{std}}^2\ (7.43 - 0.53\ NS^2) + SP_{std}(1.06\ NS^2 - 2.47\ NS) \qquad (13)$$

$$SP\ B:\ \ CoV = 6.51 + 0.8NS^2 + {SP_{std}}^2(-5.38 - 0.53NS^2) + SP_{std}(1.06NS^2 - 2.47NS) \qquad (14)$$

Equations (13) and (14) are represented as contour plots in **Fig. 10**. In pastes with SP A, compressive strength variability was generally higher than 6%. The lowest CoV values observed in pastes with SP A corresponded to mixes with NS contents higher than 3%, which fall outside the limits of the compatibility region as per **Fig. 6**. In consequence, it was not possible to simultaneously maximize the flowability and minimize the variability of compressive strength in pastes with NS and SP A. In contrast, when pastes produced with NS and SP B were considered, it was possible to identify different combinations of NS content and SP dosage for which the variability of compressive strength was low and the flowability was high, as CoV values were lower than 6% for a wide range of proportionings within the limits of the compatibility region as per **Fig. 6**. In particular, CoV values could be reduced to less than 2% even in mixes with NS contents up to 2% as long as the SP B dosage was at the higher end of its range of recommended dosages. Furthermore, these cases included those combinations that maximized the average compressive strength. This confluence of highest compressive strength, lowest variability and high flowability confirms that the concept of compatibility, although its definition is based on fresh performance criteria, is also relevant to the performance of pastes in their hardened state.

Compatibility and optimization: closing remarks

The analysis presented in the previous sections can be summarized in three conclusions: a) from the point of view of fresh state performance, SP A was found to be less compatible with cement and NS than SP B; b) the level of NS contents required to maximize compressive strength was higher for pastes made with SP A instead of SP B; c) in terms of compressive strength variability, mixes with SP B yielded better results than those with SP A. These three perspectives (flowability, compressive strength, and variability) can be put together by plotting the true compatibility regions derived from equations (7) and (8) together with the optima obtained in equations (11) and (12) and the contour lines corresponding to CoV less than 6% from **Fig. 10**. This is shown in **Fig. 11** and **12**. **Fig. 11** shows that, in the case of pastes made with SP A, the condition of maximum compressive strength (NS = 2.87%) was outside the true compatibility region, and therefore it could not be reached at the same time a good level of flowability was maintained. On the other hand, **Fig. 12** shows that in the case of pastes made with SP B, which was more compatibile with NS than SP A, the double line maximizing compressive strength fell within the true compatibility region, and therefore pastes made with NS and SP B with good flowability and maximum compressive strength were achievable.

It can be concluded that when a more compatible SP is used, the amount of NS needed to maximize the compressive strength is reduced, which means that costs directly associated to the consumption of NS can be minimized whilst improving compressive strength at the same time. In other words, utilizing a highly compatible SP can yield better mechanical performance at a lower cost, meaning that the introduction of NS at relatively low dosages in a highly compatible NS-cement-SP system effectively reduces the unit cost of each MPa gained in strength. In conclusion, the cost-effectiveness of the addition of NS to cement-based materials appears inextricably linked to its compatibility with the SP used, and does not necessarily imply the need for higher NS contents.

SUMMARY AND CONCLUSIONS

1. A new methodology based on the Marsh funnel test and compressive strength has been proposed, applicable to the assessment of interactions between superplasticizers and nanosilica in cement-based materials.
2. The effect of two different superplasticizers (SP A and SP B) at three different dosages (0.3%, 0.4% and 0.5% for SP A, and 0.6%, 0.8% and 1.0% for SP B) has been examined in cement pastes with different nanosilica contents (0%, 0.5%, 2.0%, and 3.0%) in terms of flowability, compressive strength, and variability. The corresponding equations have been obtained for these three parameters by means of multiple linear regression.
3. For the quantitative analysis of the Marsh funnel test results, the inverse of the flow time $1/t_{1000}$ is a more useful parameter than the untransformed t_{1000}, as it makes it possible to account for pastes that are too thick to flow, for which $1/t_{1000} = 0$ can be assumed.
4. The concept of region of true compatibility has been introduced, allowing for systematic comparisons between different superplasticizers regarding their effectiveness in maintaining adequate levels of flowability of pastes with nanosilica. The applicability of this concept to cost-benefit optimization has been demonstrated.
5. The differences between the superplasticizers considered, in terms of their effect on the flowability of cement pastes with nanosilica contents up to 0.5%, are negligible as long as they are dosed within their recommended ranges. Within that range,

increasing their dosage has little impact on flowability for nanosilica contents up to 1.5%.

6. The addition of nanosilica in doses of 1.5% or higher significantly reduces flowability. The maximum nanosilica content that can be added to a cement paste without making it too thick to flow through the Marsh funnel has been introduced as a reference parameter to compare different superplasticizers.
7. Increasing the nanosilica content significantly improves compressive strength. When the less compatible SP is used, the strength gain is particularly noticeable but its optimization is not possible without compromising the flowability of the paste.
8. The optimization of cement pastes with nanosilica in terms of flowability, compressive strength and low variability is only feasible when the superplasticizer used is highly compatible. A careful selection of the superplasticizer proves critical to ensuring that the addition of nanosilica is cost-effective.

ACKNOWLEDGMENTS

The authors wish to thank the companies Ecocem, Basf and AkzoNobel for providing them with the materials used in this research.

REFERENCES

1. Sonebi, M., Bassuoni, M.T., Kwasny, J., and Amanuddin, A.K., "Effect of Nanosilica on Rheology, Fresh Properties, and Strength of Cement-Based Grouts", Journal of Materials in Civil Engineering, V. 27, No. 4, April 2015, pp. 04014145-1-04014145-11 .

2. Svermova, L., Sonebi, M., and Bartos, P.J.M., “Influence of mix proportions on rheology of cement grouts containing limestone powder”, Cement and Concrete Composites, V. 25, No. 7, Oct. 2003, pp. 737-749.

3. Jalal, M., Pouladkhan, A., Harandi, O.F., and Jafari, D., “Comparative study on effects of Class F fly ash, nano silica and silica fume on properties of high performance self compacting concrete”, Construction and Building Materials, V.94, Sep. 2015, pp. 90-104.

4. Barcelo, L., Kline, J., Walenta, G., and Gartner, E., “Cement and carbon emissions”, Materials and Structures, V. 47, No. 6, Jun 2014, pp. 1055-65.

5. Feynman, R.P., “There’s plenty of room at the bottom”, Engineering and Science, V. 23, 1960, pp. 22-36.

6. Sanchez, F., and Sobolev, K., “Nanotechnology in concrete - A review”, Construction and Building Materials, V. 24, No. 11, 2010, pp. 2060-2071.

7. Pacheco-Torgal, F., and Jalali, S., “Nanotechnology: Advantages and drawbacks in the field of construction and building materials”, Construction and Building Materials, V. 25, No. 2, 2011, pp. 582-590.

8. Meng, T., Yu, Y., Qian, X., Zhan, S., and Qian, K., “Effect of nano-TiO_2 on the mechanical properties of cement mortar”, Construction and Building Materials, V. 29, Apr. 2012, pp. 241-245.

9. Berra, M., Carassiti, F., Mangialardi, T., Paolini, A.E., and Sebastiani, M., “Effects of nanosilica addition on workability and compressive strength of Portland cement pastes”, Construction and Building Materials, V. 35, Oct. 2012, pp. 666-675.

10. Biricik, H., and Sarier, N., “Comparative study of the characteristics of nano silica- , silica fume- and fly ash- incorporated cement mortars”, Materials Research, V. 17, No. 3, May 2014, pp. 570-582.

11. Kawashima, S., Hou, P., Corr, D.J., and Shah, S.P., “Modification of cement-based materials with nanoparticles”, Cement and Concrete Composites, V. 36, Feb. 2013, pp. 8-15.

12. Singh, L.P., Karade, S.R., Bhattacharyya, S.K., Yousuf, M.M., and Ahalawat, S., “Beneficial role of nanosilica in cement based materials - A review”, Construction and Building Materials, V. 47, 2013, pp. 1069-1077.

13. Sobolev, K., Flores, I., Hermosillo, R., and Torres-Martínez, L.M., “Nanomaterials and nanotechnology for high-performance cement composites”, ACI Special Publication 254, Jan. 2008, pp. 93-120.

14. Sobolev, K., Flores, I., Torres-Martinez, L.M., Valdez, P.L., Zarazua, E., and Cuellar, E.L., “Engineering of SiO_2 Nanoparticles for Optimal Performance in Nano Cement-Based Materials”, Proceedings of NICOM3 Nanotechnology in Construction 3, Jun. 2009, pp. 139-148.

15. Zapata, L.E., Portela, G., Suárez, O.M., and Carrasquillo, O., “Rheological performance and compressive strength of superplasticized cementitious mixtures with micro/nano-SiO2 additions”, Construction and Building Materials, V. 41, 2013, pp. 708-716.

16. Konsta-Gdoutos, M.S., “Nanomaterials in self-consolidating concrete: a state-of-the-art review”, Journal of Sustainable Cement-Based Materials, V. 3, No. 3-4, pp. 167-180.

17. Abd El Aleem, S., Heikal, M., and Morsi, W.M., "Hydration characteristic, thermal expansion and microstructure of cement containing nano-silica", Construction and Building Materials, V. 59, May 2014, pp. 151-160.

18. Garcia-Taengua, E., Sonebi, M., Hossain, K.M.A., Lachemi, M., and Khatib, J., "Effects of the addition of nanosilica on the rheology, hydration and development of the compressive strength of cement mortars", Composites Part B: Engineering, V. 81, 2015, pp. 120-129.

19. Qing, Y., Zenan, Z., Deyu, K., and Rongshen, C., "Influence of nano-SiO2 addition on properties of hardened cement paste as compared with silica fume", Construction and Building Materials, V. 21, No. 3, 2007, pp. 539-545.

20. Senff, L., Hotza, D., Lucas, S., Ferreira, V.M., and Labrincha, J.A., "Effect of nano-SiO_2 and nano-TiO_2 addition on the rheological behavior and the hardened properties of cement mortars", Materials Science and Engineering, V. 532, Jan. 2012, pp. 354-561.

21. Sonebi, M., García-Taengua, E., Hossain, K.M.A., Khatib, J., and Lachemi, M., "Effect of nanosilica addition on the fresh properties and shrinkage of mortars with fly ash and superplasticizer", Construction and Building Materials, V. 84, Jun. 2015, pp. 269-276.

22. Horszczaruk, E., Mijowska, E., Cendrowski, K., Mijowska, S., and Sikora, P., "Effect of incorporation route on dispersion of mesoporous silica nanospheres in cement mortar", Construction and Building Materials, V. 66, 2014, pp. 418-421.

23. De Rojas, M.I.S., and Frías, M., "The pozzolanic activity of different materials, its influence on the hydration heat in mortars", Cement and Concrete Research, V. 26, No. 2, Feb. 1996, pp. 203-213.

24. Senff, L., Labrincha, J.A., Ferreira, V.M., Hotza, D., and Repette, W.L., "Effect of nano-silica on rheology and fresh properties of cement pastes and mortars", Construction and Building Materials, V. 23, No. 7, Jul. 2009, pp. 2487-2491.

25. Kong, D., Corr, D.J., Hou, P., Yang, Y., and Shah, S.P., "Influence of colloidal silica sol on fresh properties of cement paste as compared to nano-silica powder with agglomerates in micron-scale", Cement and Concrete Composites, V. 63, 2015, pp. 30-41.

26. Burgos-Montes, O., Palacios, M., Rivilla, P., and Puertas, F., "Compatibility between superplasticizer admixtures and cements with mineral additions", Construction and Building Materials, V. 31, Jun. 2012, pp. 300-309.

27. Nehdi, M., Mindess, S., and Aïtcin, P.C., “Optimization of high strength limestone filler cement mortars”, Cement and Concrete Research, V. 26, No. 6, 1996, pp. 883-893.

28. Jolicoeur, C., and Simard, M.A., “Chemical admixture-cement interactions: Phenomenology and physico-chemical concepts”, Cement and Concrete Composites, V. 20, No. 2-3, Jan. 1998, pp. 87-101.

29. Agulló, L., Toralles-Carbonari, B., Gettu, R., and Aguado, A., “Fluidity of cement pastes with mineral admixtures and superplasticizer - A study based on the Marsh cone test”, Materials and Structures, V. 32, No. 7, Aug. 1999, pp. 479-485.

30. European Committee for Standardization, “EN 196-1:2016 Methods of testing cement. Determination of Strength”, 2016, 38 pp.

31. European Committee for Standardization, “EN 445:2007 Grout for prestressing tendons. Test methods”, 2007, 18 pp.

32. Garcia-Taengua, E., Sonebi, M., Taylor, S., Ferrara, L., Deegan, P., and Pattarini, A., “Compatibility of superplasticizers with cementitious materials”, BFT International, V. 80, No. 10, Oct. 2014, pp. 44-53.

33. European Committee for Standardization, “EN 12390-3:2009 Testing hardened concrete - Part 3: Compressive strength of test specimens”, 2009, 22 pp.

TABLES AND FIGURES

List of Tables:

List of Figures:

Table 1–Variables and values considered

Variables		Levels of variation		
SP Type		SPA, SPB		
SP dosage	SPA	0.3%	0.4%	0.5%
	SPB	0.6%	0.8%	1.0%
	Typified	-1	0	+1
NS content		0.5%, 2.0%, 3.5%		

Table 2–Marsh funnel test results

NS (%)	SP Type	SP (%)	t_{1000} (seconds)	$1/t_{1000}$
0.0	A	0.3	16.8	0.0595
0.0	A	0.4	16.2	0.0617
0.0	A	0.5	15.1	0.0662
0.5	A	0.3	21.2	0.0472
0.5	A	0.4	18.0	0.0556
0.5	A	0.5	19.4	0.0515
2.0	A	0.3	41.8	0.0239
2.0	A	0.4	35.5	0.0282
2.0	A	0.5	21.1	0.0474
3.5	A	0.3	(*)	0.0000
3.5	A	0.4	(*)	0.0000
3.5	A	0.5	(*)	0.0000
0.0	B	0.6	10.5	0.0952
0.0	B	0.8	10.1	0.0990
0.0	B	1.0	9.8	0.1020
0.5	B	0.6	12.3	0.0813
0.5	B	0.8	10.6	0.0943
0.5	B	1.0	12.5	0.0800
2.0	B	0.6	25.9	0.0386
2.0	B	0.8	14.9	0.0671
2.0	B	1.0	16.7	0.0599
3.5	B	0.6	(*)	0.0000
3.5	B	0.8	(*)	0.0000
3.5	B	1.0	24.9	0.0402

(*): Cases where the grout was too thick to flow.

Table 3–Compressive strength results

NS (%)	SP Type	SP (%)	Compressive strength		
			Average, MPa (psi)	Standard deviation, MPa (psi)	CoV(%)
0.0	A	0.3	35.3 (5119.8)	4.3 (623.7)	12.2
0.0	A	0.4	33.8 (4902.3)	2.1 (304.6)	6.2
0.0	A	0.5	36.6 (5308.4)	5.2 (754.2)	14.2
0.5	A	0.3	32.9 (4771.8)	5.0 (725.2)	15.2
0.5	A	0.4	45.8 (6642.7)	2.8 (406.1)	6.1
0.5	A	0.5	38.4 (5569.5)	5.3 (768.7)	13.8
2.0	A	0.3	51.7 (7498.5)	7.6 (1102.3)	14.7
2.0	A	0.4	48.9 (7092.4)	1.4 (203.1)	2.9
2.0	A	0.5	55.0 (7977.1)	6.4 (928.2)	11.6
3.5	A	0.3	57.6 (8354.2)	1.7 (246.6)	2.9
3.5	A	0.4	54.8 (7948.1)	6.1 (884.7)	11.1
3.5	A	0.5	63.6 (9224.4)	6.0 (870.2)	9.4
0.0	B	0.6	48.5 (7034.3)	0.6 (87.0)	1.3
0.0	B	0.8	52.1 (7556.5)	3.4 (493.1)	6.5
0.0	B	1.0	55.3 (8020.6)	0.3 (43.5)	0.6
0.5	B	0.6	58.2 (8441.2)	1.4 (203.1)	2.4
0.5	B	0.8	66.5 (9645.0)	6.0 (870.2)	9.0
0.5	B	1.0	67.1 (9732.0)	0.2 (29.0)	0.3
2.0	B	0.6	71.8 (10413.7)	0.6 (87.0)	0.8
2.0	B	0.8	63.2 (9166.4)	4.8 (696.2)	7.6
2.0	B	1.0	71.7 (10399.2)	0.7 (101.5)	1.0
3.5	B	0.6	64.4 (9340.4)	0.3 (43.5)	0.5
3.5	B	0.8	62.8 (9108.4)	9.8 (1421.4)	15.6
3.5	B	1.0	64.6 (9369.5)	7.5 (1087.8)	11.6

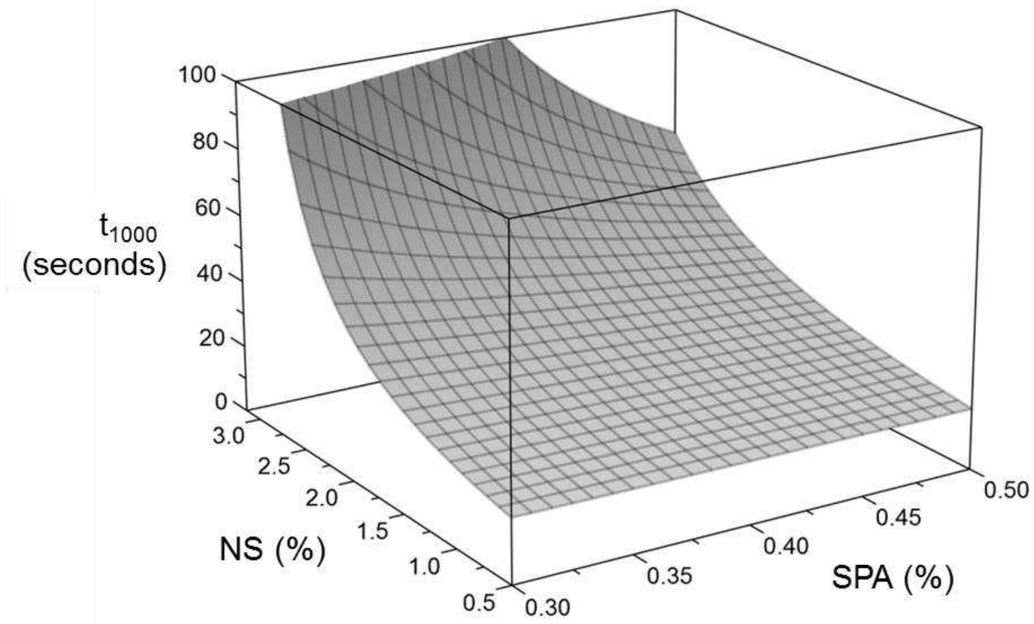

Fig. 1–Flow time vs nanosilica and SPA dosage.

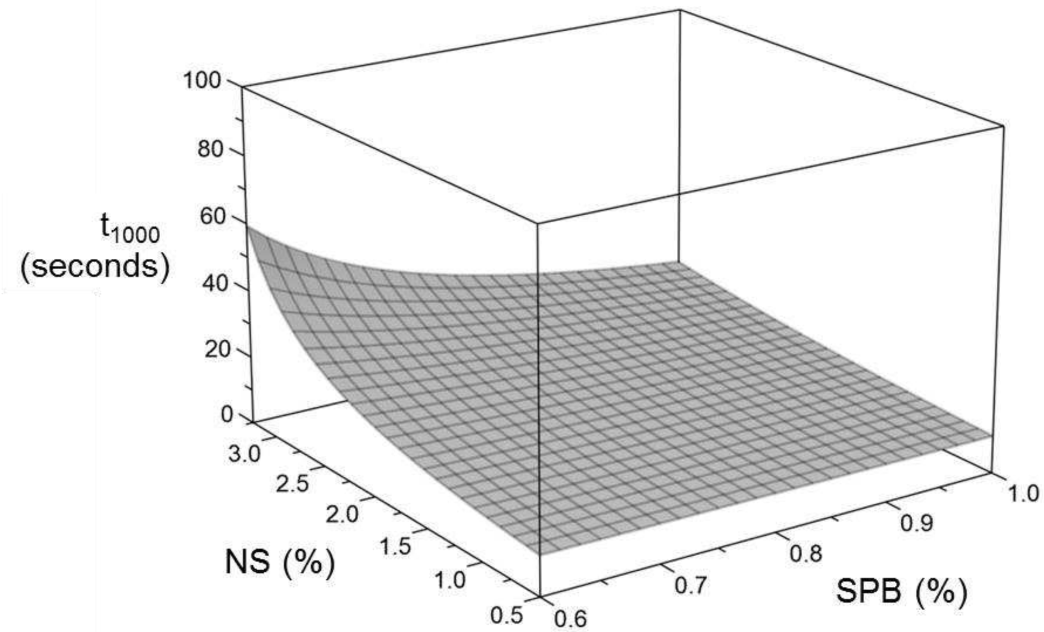

Fig. 2–Flow time vs nanosilica and SPB dosage.

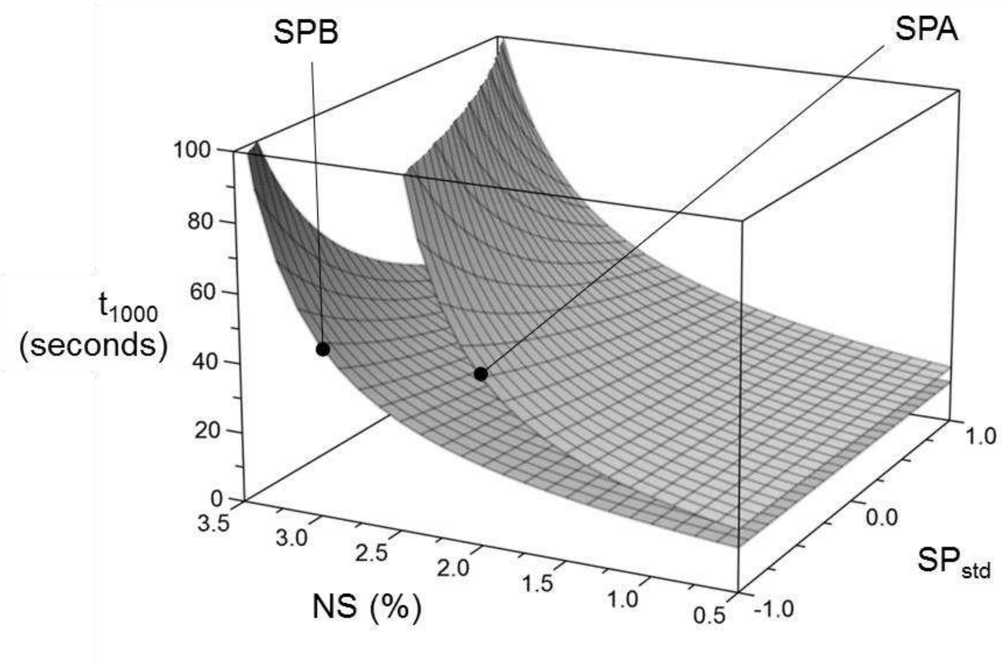

Fig. 3–Flow time vs NS content and typified SP dosage.

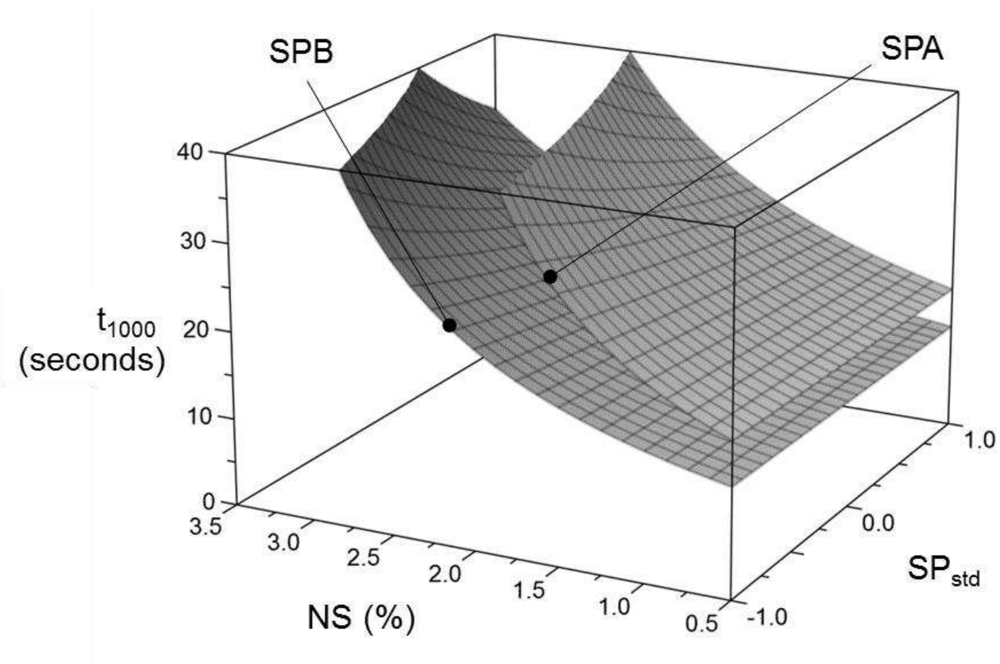

Fig. 4–Flow time vs NS content and typified SP dosage, capped at 40 seconds.

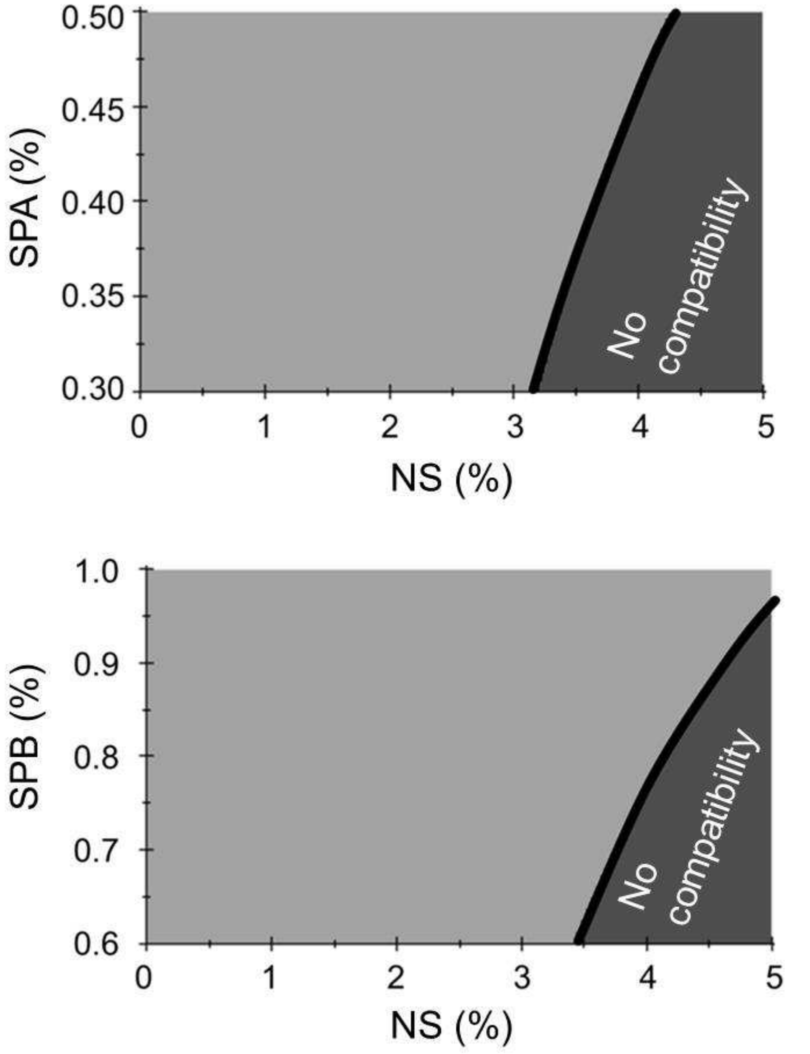

Fig. 5–Compatibility regions for NS-SPA (above) and NS-SPB (below).

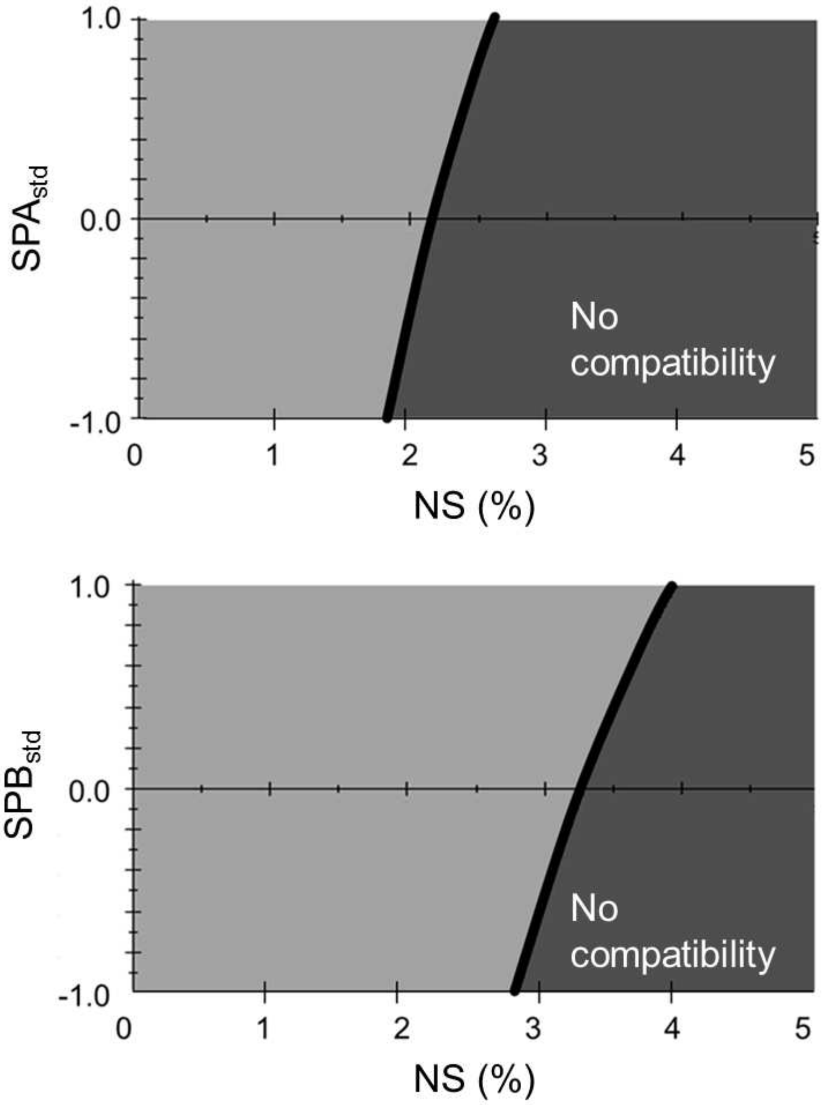

Fig. 6–True compatibility regions for NS-SPA (above) and NS-SPB (below).

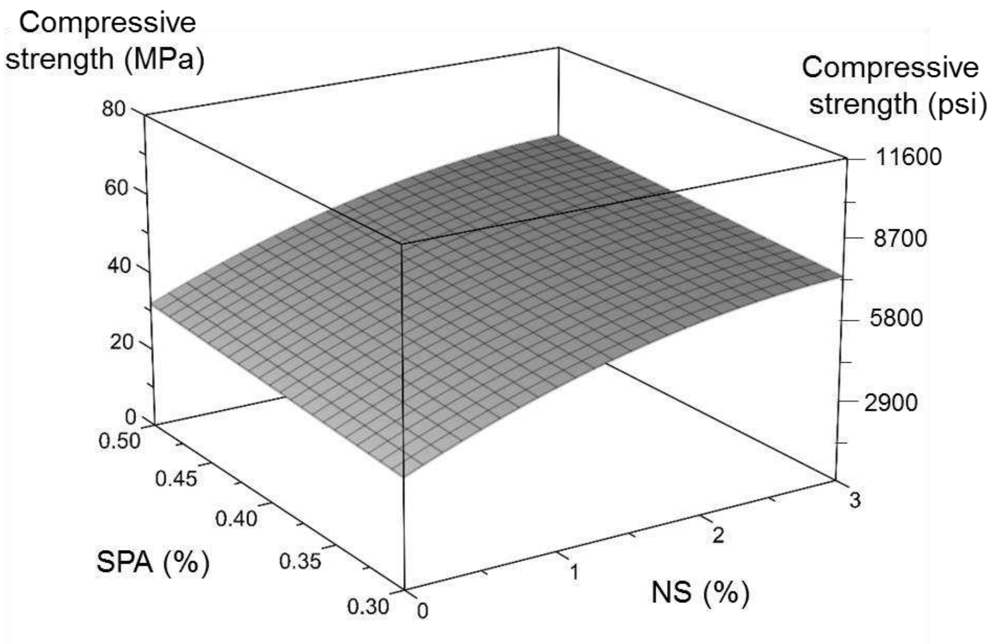

Fig. 7–Average compressive strength of NS-SPA mixes.

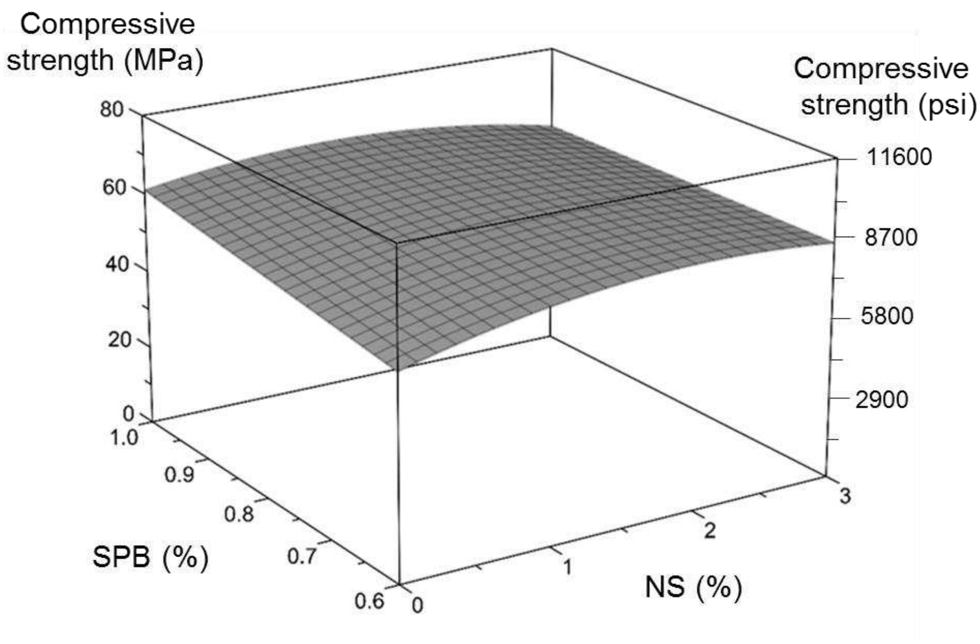

Fig. 8–Average compressive strength of NS-SPB mixes.

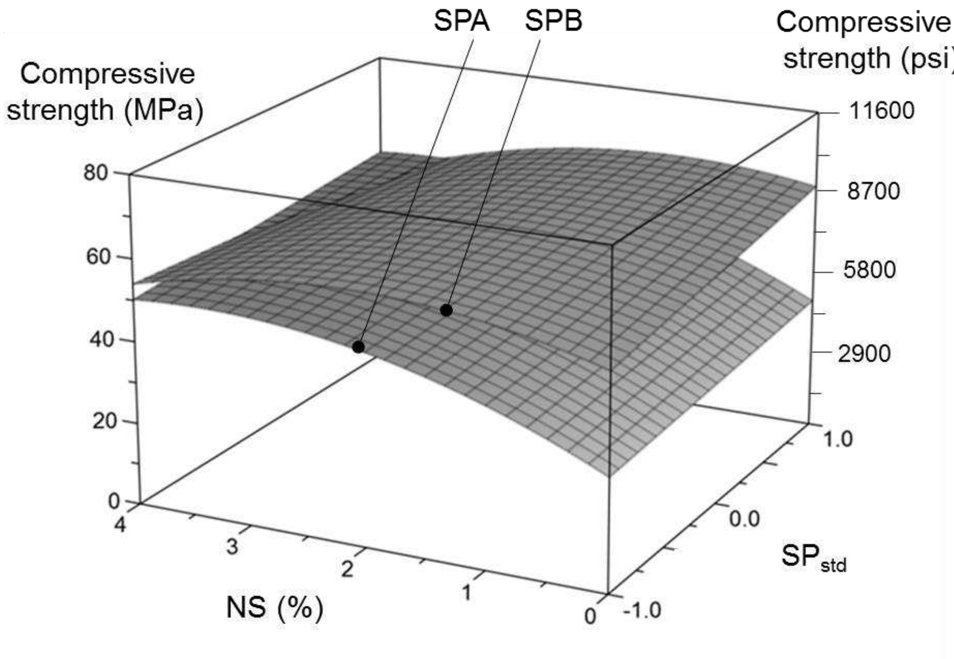

Fig. 9–Average compressive strength vs NS content and typified SPA, SPB dosages.

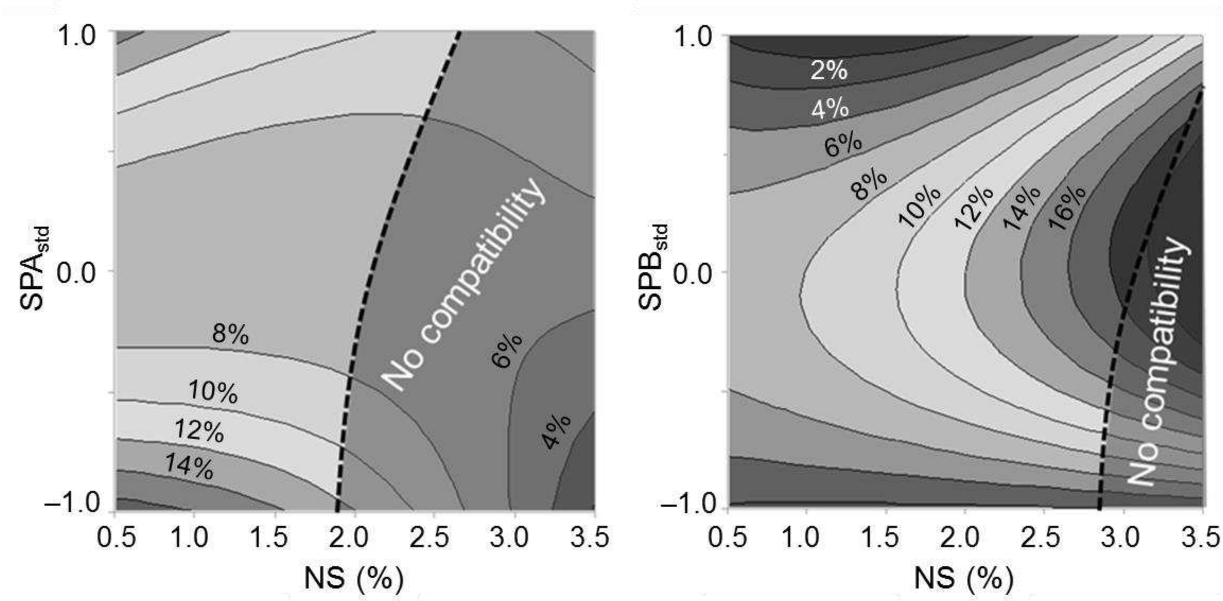

Fig. 10–Coefficient of variation for compressive strength vs NS content and typified SPA, SPB dosages.

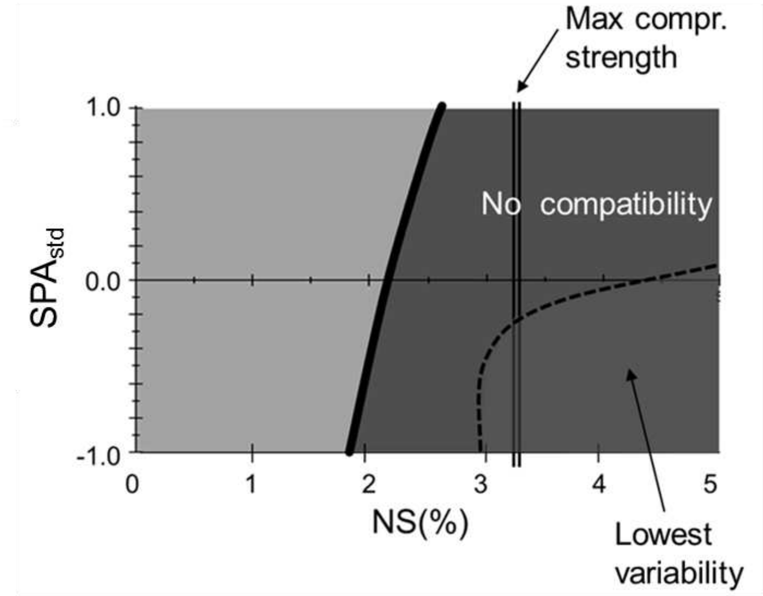

Fig. 11– True compatibility region and compressive strength optimization of NS-SPA mixes.

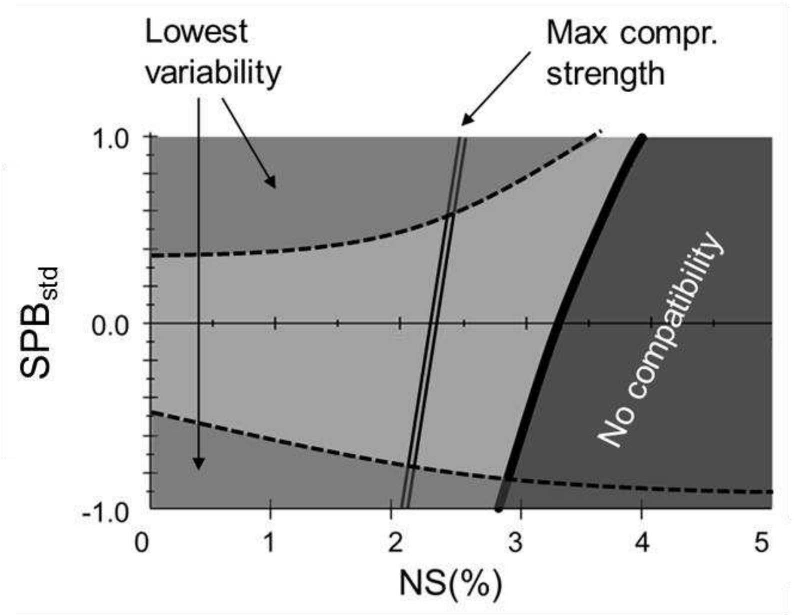

Fig. 12– True compatibility region and compressive strength optimization of NS-SPB mixes.